NeuroImage: Clinical 4 (2014) 668–675

Contents lists available at ScienceDirect

NeuroImage: Clinical

journal homepage: www.elsevier.com/locate/ynicl

Patient-specific connectivity pattern of epileptic network in frontal lobe epilepsy

Cheng Luo[a,b,*], Dongmei An[a,c], Dezhong Yao[b], Jean Gotman[a]

[a]Montreal Neurological Institute, McGill University, Montreal, Quebec, Canada
[b]Key Laboratory for Neuroinformation of Ministry of Education, School of Life Science and Technology, University of Electronic Science and Technology of China, Chengdu, China
[c]Department of Neurology, West China Hospital of Sichuan University, Chengdu, China

ARTICLE INFO

Article history:
Received 20 December 2013
Received in revised form 1 April 2014
Accepted 13 April 2014

Keywords:
Frontal lobe epilepsy
fMRI
Functional connectivity
Epileptic network

ABSTRACT

There is evidence that focal epilepsy may involve the dysfunction of a brain network in addition to the focal region. To delineate the characteristics of this epileptic network, we collected EEG/fMRI data from 23 patients with frontal lobe epilepsy. For each patient, EEG/fMRI analysis was first performed to determine the BOLD response to epileptic spikes. The maximum activation cluster in the frontal lobe was then chosen as the seed to identify the epileptic network in fMRI data. Functional connectivity analysis seeded at the same region was also performed in 63 healthy control subjects. Nine features were used to evaluate the differences of epileptic network patterns in three connection levels between patients and controls. Compared with control subjects, patients showed overall more functional connections between the epileptogenic region and the rest of the brain and higher laterality. However, the significantly increased connections were located in the neighborhood of the seed, but the connections between the seed and remote regions actually decreased. Comparing fMRI runs with interictal epileptic discharges (IEDs) and without IEDs, the patient-specific connectivity pattern was not changed significantly. These findings regarding patient-specific connectivity patterns of epileptic networks in FLE reflect local high connectivity and connections with distant regions differing from those of healthy controls. Moreover, the difference between the two groups in most features was observed in the strictest of the three connection levels. The abnormally high connectivity might reflect a predominant attribute of the epileptic network, which may facilitate propagation of epileptic activity among regions in the network.

1. Introduction

Epilepsy is characterized by abnormal neuro-electrical activity in the brain. In focal seizures and focal epilepsy the epileptic activity arises primarily within networks limited to one hemisphere. The origin of focal seizures may be associated with the localization of radiologically visible brain lesions or electrophysiological abnormalities. However, there is growing evidence from neuroimaging that focal epilepsies involve an abnormal functional network rather than a single epileptogenic region (Kramer and Cash, 2012; Constable et al., 2013; Laufs, 2012). Using combined EEG and fMRI recordings (EEG/fMRI), our group showed that focal interictal epileptic discharges (IEDs) are associated with specific networks of widespread metabolic changes in different focal epilepsies (Fahoum et al., 2012). The abnormal neuronal activity in epileptic networks may lead to interictal and ictal epileptic activity. Therefore, the characteristic of the epileptic network may be important to assess seizure initiation or propagation.

Recently, functional connectivity (FC) analysis based on resting state fMRI has revealed more than ten reproducible brain networks in healthy controls. Disturbed FC maps are observed in different types of epilepsy and are associated with cognitive impairment and propagation of epileptic activity (Bettus et al., 2009; Vaessen et al., 2013; Liao et al., 2011; Luo et al., 2012; Zhang et al., 2011). Seed-based FC analysis can identify the remote regions connected with the seed. For example, the motor network can be defined when the seed is placed at the primary motor cortex (Biswal et al., 1995). Using this approach, we demonstrated abnormal FC in some resting state functional networks in generalized epilepsy (Luo et al., 2011; Maneshi et al., 2012). The FC map seeded at the epileptogenic focus might provide a window to investigate seizure initiation and propagation. For example, FC seeded at the hippocampus was used to identify the lateralization of temporal lobe epilepsy (TLE) (Morgan et al., 2012), and to identify abnormal connectivity in this condition (Pittau et al., 2012). EEG/fMRI may provide a priori information useful to define part of the epileptic network, because it can help delineate epileptogenic regions

* Corresponding author.
E-mail address: chengluo@uestc.edu.cn (C. Luo).

2213-1582/$ - see front matter
http://dx.doi.org/10.1016/j.nicl.2014.04.006

non-invasively, by pointing to regions where there are hemodynamic changes correlated with the epileptic activity as detected on EEG. FC analysis based on EEG/fMRI findings has been performed in previous studies.

Most of these FC analysis studies investigate the differences between two groups in the strength of voxel-based FC with the potential epileptogenic region, such as FC with the hippocampus in patients with TLE and in controls (Pittau et al., 2012). However, it is difficult to perform FC strength analysis in a group of epileptic patients with epileptic foci in different regions, because the seeds of FC are different for each patient. The pattern of FC, i.e. the distribution of FC regions rather than the strength of FC would be another attribute to delineate interaction between the seed and other regions in the brain. For example, the symmetry of FC map is often evaluated as a spatial feature. The lateralized index of FC maps may predict surgical outcome for candidates of epileptic surgery (Negishi et al., 2011). Specific brain regions in epileptic network are associated with seizure initiation or propagation, with their activity modulating or modulated by the occurrence of epileptic activity. Therefore, the patterns of FC seeded at a given brain structure could be different between patients and controls. Evaluating the characteristics of FC patterns would help uncover the difference between patient-specific pathways and normal pathway in control subjects, and provide detailed information to understand the connectivity of a particular epileptogenic region.

In the current study, we investigate the patterns of epileptic networks in a group of patients with frontal lobe epilepsy (FLE), using the FC map seeded at the epileptogenic regions defined by EEG/fMRI. We hypothesize that epileptic networks are reflected in patient-specific pathways different from the FC maps seeded at the same region in healthy controls.

2. Materials and methods

2.1. Participants

Between April 2006 and September 2012, 41 patients with frontal lobe epilepsy were evaluated with 3 T EEG–fMRI scans at the Montreal Neurological Institute and Hospital (MNI/MNH). The diagnosis was established according to the diagnostic criteria published by the International League Against Epilepsy (Engel, 2001). Only patients without distinct structural brain abnormality, such as atrophy caused by surgery or injury, tumor, or significant malformation of cortical development leading to distortion of brain anatomy, were included in the functional connectivity analysis. Therefore, patients with minor structural abnormalities such as focal cortical dysplasia consisting of a trans-mantle sign or a localized cortical thickening were included. Sixty-three age- and gender- matched healthy controls were also included in the current study, and they underwent a resting state fMRI scan. The study was approved by the Research Ethics Board of MNI/MNH. Written informed consent as approved by the MNI/MNH Research Ethics Committee was obtained from all subjects.

2.2. Data acquisition

EEG was recorded inside a 3 Tesla MRI scanner (Trio; Siemens, Germany) with 25 MR compatible scalp electrodes placed according to 10–20 (reference FCz) and 10–10 (F9, T9, P9, F10, T10, P10) systems, using a BrainAmp system (Brain Products, Munich, Germany, 5 kHz sampling). A T1-weighted anatomic image was acquired first using the following sequences: until July 2008: 1-mm slice thickness; 256 × 256 matrix; echo time (TE) 7.4 ms; repetition time (TR) 23 ms; flip angle 30°; from July 2008: 1-mm slice thickness; 256 × 256 matrix; TE 4.18 ms; TR 23 ms; flip angle 9°. T1 image was used for superimposition with functional images. Functional data were collected in 6-min runs lasting 60–90 min, with a T2*-weighted echo planar imaging (EPI) sequence: until July 2008: TR 1.75 s; TE 30 ms; 64 × 64 matrix; 25 slices; voxel 5 × 5 × 5 mm; flip angle 90° and from July 2008: TR 1.9 s; TE 25 ms; 64 × 64 matrix; 33 slices; voxel 3.7 × 3.7 × 3.7 mm; flip angle 90°. This MR protocol was used for all patients and for 25 healthy controls; the control subjects had no EEG. The remaining 38 of the 63 healthy controls were scanned in a 3 Tesla MRI scanner (GE Discovery MR750). T1-weighted image was collected using the following parameters: 1-mm slice thickness; 256 × 256 matrix; TE 1.98 ms; TR 6.008 ms; flip angle 90°. Resting state functional data with 205 volumes were acquired using gradient-echo EPI sequence (TR 2 s; TE 30 ms; 64 × 64 matrix; 33 slices; voxel 3.7 × 3.7 × 3.7 mm; flip angle 90°). The first five volumes were discarded to ensure magnetic field stabilization.

2.3. EEG and EEG/fMRI processing

The method is identical to that used in prior studies (Fahoum et al., 2012; Pittau et al., 2012). BrainVision Analyzer was used to remove MR gradient artifacts. The ballistocardiographic artifact was removed with independent component analysis (Benar et al., 2003). IEDs similar to those obtained outside the scanner were marked. IEDs were separated according to different spatial distributions, and events with different distributions were analyzed independently. Then, fMRI images were motion corrected and smoothed (6-mm full width at half maximum). Temporal autocorrelations were accounted for by fitting an autoregressive model of order 1, and low frequency drifts were modeled with a third-order polynomial fitting to each run. Timing and duration of each IED were built as a regressor and convolved with four hemodynamic response functions (HRFs) peaking at 3, 5, 7, and 9 s (Bagshaw et al., 2004). Six motion parameters were modeled as confounds. A statistic t map was created for each regressor of interest (IED or event type) using the other regressors as confounds for each event type. A combined t map was created by taking, at each voxel, the maximum t value from the four t maps based on the four HRFs. The single combined t map was used for determination of the seed. To be significant, activation required five contiguous voxels having a t value >3.1 corresponding to $p < 0.001$, corrected for multiple comparisons. Responses outside the cerebral cortex were excluded.

In addition, based on simultaneous EEG recordings, patients were divided into those in whom all runs had IEDs and those in whom at least one run had no IED. In the patients having at least one run without IEDs, we compared runs with and without IEDs, as described below.

2.4. Functional connectivity analysis

Patients who had IEDs inside the scanner and showed activation to IEDs resulting from the EEG/fMRI analysis were included in the following analysis. The activation was identified and selected as the seed according to the following criteria: (i) the seed was centered at the local maximum activation located in frontal regions or anterior cingulate cortex and ipsilateral to the maximum spike amplitude in the EEG; and (ii) the seed was shaped by the cluster of significant voxels found with EEG/fMRI. The number of voxels in the seed was limited to less than 200, because a seed larger than 200 voxels might increase the variability of time signals within the seed. This threshold is of course somewhat arbitrary. If the size of the cluster around the local maximum defined in (i) was larger than 200, the threshold was gradually increased until the size of the seed became smaller than 200; (ii) if more than one type of IEDs are present in a patient, one seed is selected for each spike type. If two such seeds overlap in a patient, they are merged.

For FC analysis, two runs were analyzed for each patient: one run with IEDs and one without IED if such a run could be found. The fMRI datasets were preprocessed with the SPM8 software package [Statistical Parametric Mapping, http://www.fil.ion.ucl.ac.uk/spm]. Slice

time correction, 3D motion detection and correction, spatial normalization to the MNI template, and spatial smoothing using an isotropic Gaussian kernel (8 mm full width at half maximum) were performed. Two procedures were used to remove physiological noise from the pre-processed time series: (i) the time series were corrected through linear regression for the effect of the six head motion parameters, and the signals from cerebrospinal fluid region, white matter region and global brain signal; and (ii) temporal band-pass filtering (pass band 0.01–0.1 Hz) was performed using a phase-insensitive filter, which reduces the effects of low-frequency drift and high-frequency noise. Resting state fMRI data from 63 healthy controls was also processed in the same way.

The time courses were averaged across voxels in a given seed. Pearson's correlation coefficient (CC) was computed between the seed time course and the time courses of all brain voxels. The CC was normalized to *z*-scores with Fisher's r-to-z transformation. For a given seed, one FC image was obtained for the corresponding patient and 63 FC images were obtained for the control subjects.

2.5. FC map characteristic analysis

In order to determine the network pattern, FC images were binarized as follows. The voxels having significant correlation with the seed were set to 1, and to 0 otherwise. To define the significance level of CC with the seed, the probability distribution of *z*-scores of CCs was obtained across voxels and subjects (including 63 controls and one patient for each seed), and the values of CC resulting from the cumulative distribution function of the statistic under the null hypothesis corresponded to $p < k$ (with cluster size >10 voxels (Friston et al., 1994)) was chosen. Because there is no gold standard to determine the threshold k, a set of thresholds ($k = 0.05, 0.01$, and 0.001) was used to identify the FC maps representing low-, middle- and high-level CC for each seed and each subject. With these thresholds, we will compare patients and control subjects. In some comparisons, there will be a difference in high-level and a difference in low-level FC, if for instance all CCs are higher in one group than in the other. It is important to note, however, that a significant group difference with high-level FC may occur in the absence of a significant difference in low-level FC. Each level measures a different type of connectivity and these types are not independent but they are not necessarily dependent on each other. As an example, there could be a significant difference in high-level FC if two regions have many high-level CCs in one group and none in the other, but no low-level difference if the number of low-level CCs is the same in both groups (Fig. S1).

To evaluate the differences between patterns of FC in patients and controls, nine map features were determined. These features were divided into two categories depending on whether they described the individual or overlap features of the FC maps.

2.5.1. Individual FC map characteristics

The following features were used to assess the individual FC maps at the whole brain level: Feature 1, a lateralization index (LI) and Feature 2, the total number of voxels with significant correlation in the whole brain normalized by the number of voxels in the seed. Moreover, the local and remote FC regions of the seed were separated, and the local region where the seed is located was named the first cluster. Then the following two features were assessed at the cluster level: Feature 3, the number of voxels in the first cluster also normalized by the number of voxels in the seed and Feature 4, the percentage of total FC voxels located in the first cluster (Feature 2 divided by Feature 3). LI was determined with the following formula:

$$\mathrm{LI} = \frac{\text{number of voxels in ispilateral hemisphere number of voxels in contralateral hemisphere}}{\text{number of voxels in ipsilateralhemisphere} + \text{number ofvoxels in contralateral hemisphere}}.$$

To quantify the difference between patients and healthy controls, the paired *t*-test was used. For example, a seed Sm was identified in the patient Pm, the FC map (PA-S*m*) was obtained in Pm, and the FC maps (HC*n*-S*m*, $n = 1 \ldots 63$) were obtained in the control subjects. The LI was calculated for the 64 FC maps. The LI of PA-S*m* and the mean LI of 63 HC*n*-S*m* constituted a pair of values corresponding to the seed Sm. For all *m* seeds, two columns of values were therefore obtained, and then the paired sample *t*-test was performed between them. The comparison between patients and controls was performed for each of the three threshold levels, for the four "individual" features. Similarly, the same paired sample *t*-test was used to assess the difference between runs with and without IEDs for patients whose fMRI data included runs with and without IEDs.

2.5.2. Overlapping characteristics of FC maps

To understand the internal detailed features of an FC map, we analyzed the overlap between the individual FC map of a seed *m* in a patient and a template map, referred to as HC-Sm–tmap. We defined the HC-Sm–tmap as an FC template at seed *m* from healthy controls as a representation of the FC common to the healthy controls for seed *m*. In order to define this common FC, we performed a one sample *t* test for FC images in the group of healthy controls (63 subjects). The binarized *t* value with threshold $p < 0.001$ (corrected by FWE) constituted the HC-Sm–tmap. We then defined the five "overlap" features (Feature 5–9) fully defined in Fig. 1, and summarized here, Feature 5: Overlap between individual map and template, Feature 6: Proportion of overlapping voxels, Feature 7: Proportion of non-overlapping voxels, Feature 8: Percentage of overlapping voxels located in the first cluster, and Feature 9: Proportion of overlapping voxels outside the first cluster. These features were obtained for each patient (comparing PA-S*m* and HC-Sm–tmap) and for each control subject (comparing HC*n*-S*m* and HC-Sm–tmap). The paired sample *t*-test, as mentioned above, was computed for these parameters. Feature 5 and Feature 6 delineated the overlapping characteristics between individual FC maps and the template (HC-Sm–tmap) at the voxel level. Feature 7 represents the non-overlapping voxels in an individual FC map, and reflects FC present in an individual but absent in the control subjects. It may represent FC related to epileptic activity. For the cluster-level overlap measures, Feature 8 represented the percentage of overlapping voxels located in the first cluster to total overlapping voxels, and Feature 9 reflects how much of the individual map overlaps the template outside the first cluster.

2.6. Individual variance of FC map

The resting state functional connectivity pattern has variance across subjects. According to the study of Mueller et al. (2013), the correlation of FC images between subjects was used to delineate the variance of resting state FC images. For a given seed *m*, the similarity between 64 images (one PA-S*m* and 63 HC*n*-S*m*) was computed by averaging the CC between all pairs of FC images. These CCs were averaged across seeds and the resulting value was used to show the variability of FC images.

Moreover, we also divided the CCs between 64 FC images of a given seed *m* into two parts, one part included 63 CCs between one PA-S*m* and the 63 HC*n*-S*m*, the other included C_{63}^2 CCs between each pair of maps of the 63 HC*n*-S*m*. They were then averaged separately. Two groups of values were therefore obtained; a patient group representing the similarity between patients and controls, and a control group representing the similarity within controls. The paired sample *t*-test, as mentioned above, was used to evaluate the differences in the similarity of the FC images (after Fisher's r-to-z transformation). In addition, to check whether the inter-subject variance influenced all the features mentioned above, the Pearson's correlation between variance and these features was assessed in patients individually.

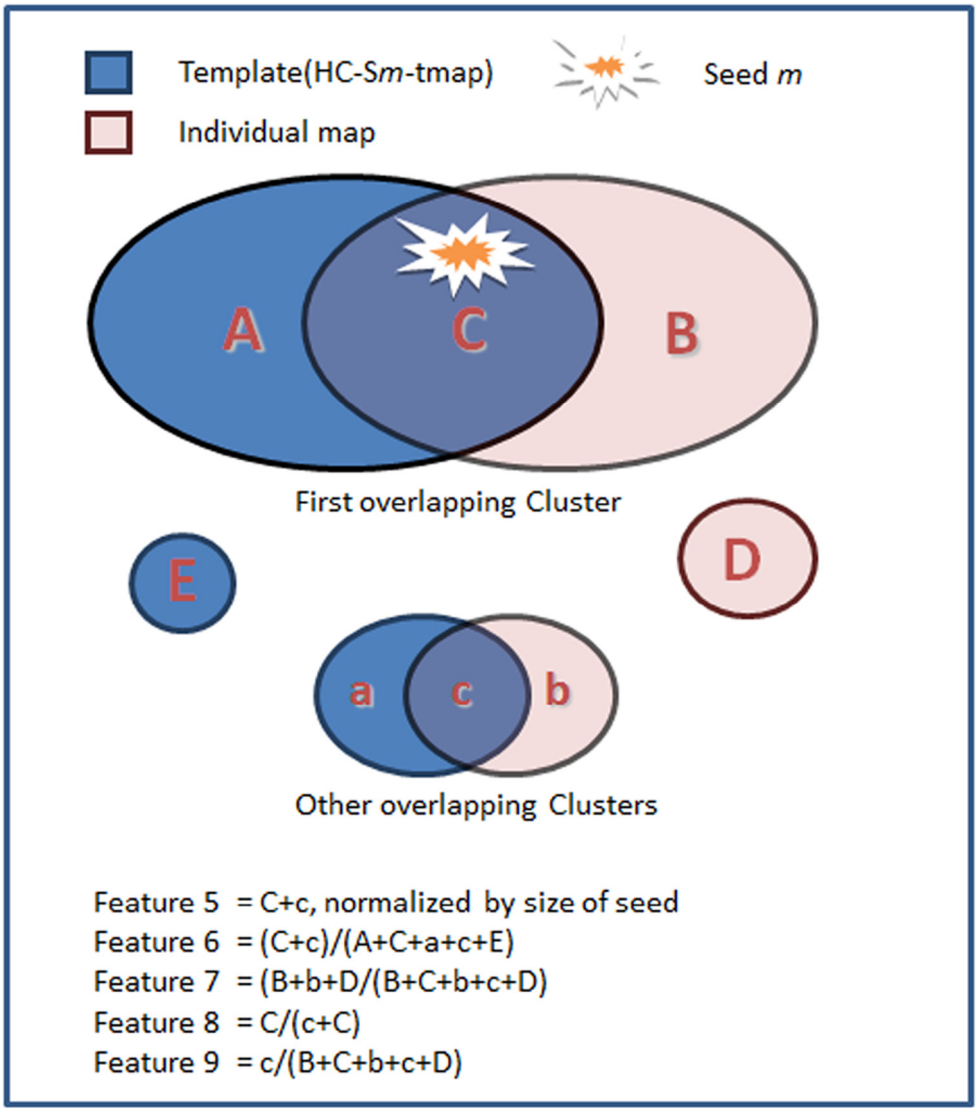

Fig. 1. Chart of overlapping characteristics between individual map and template (HC−Sm-tmap).**Feature 5**: *overlap between individual map and template* represents the number of overlapping voxels divided by the number of voxels of seed. **Feature 6**: *proportion of overlapping voxels* is the ratio of the total number of overlapping voxels to the number of significant voxels in the HC−Sm-tmap (template). **Feature 7**: *proportion of non-overlapping voxels* is the ratio of the total number of non-overlapping voxels in an individual FC map to the total number of voxels in that individual FC map. **Feature 8**: *percentage of overlapping voxels located in the first cluster* is the ratio of the number of voxels in the first overlapping cluster to the total number of overlapping voxels. **Feature 9**: *proportion of overlapping voxels outside the first cluster* is the ratio of the number of voxels in other overlapping clusters (i.e. outside the first overlapping cluster) to the number of voxels in the individual FC map.

3. Results

3.1. Identifying seeds based on EEG–fMRI findings

Forty-one patients were selected for this study. Of those, 11 revealed distinct structural lesions, one patient had no IED during fMRI scanning, 3 patients had no significant BOLD activation to their marked IEDs, and 3 patients had technical problems preventing interpretation, including significant movements during scanning, persistent EEG artifact, and loss of important EEG channels. Twenty-three patients were then included in this study (12 females; mean age, 26.22 ± 10.2 years; age of onset, 9.02 ± 7.33 years). Twenty-five seeds were selected based on significant activation regions to the epileptic spikes (two patients had two spike types, the remaining 21 patients had 1 spike type each). The seed sizes ranged from 58 to 193 voxels for the 25 seeds. Runs with and without IEDs were obtained in 13 patients, and two seeds were identified in one of them, resulting in 14 seeds and FC maps for the runs without IED.

3.2. Functional connectivity map analysis

For each seed, FC maps were calculated in the corresponding patient and in the 63 controls. According to the probability distribution of the *z*-scores of CCs across voxels and subjects for a given seed, three CC thresholds were determined. The three averaged thresholds across the 25 seeds were 0.390 for low-level ($p = 0.05$), 0.550 for middle-level ($p = 0.01$), and 0.729 for high-level ($p = 0.001$). The features of thresholded FC maps were compared between patients and controls, and between runs with and without IEDs in the patients who had both types of runs.

3.3. Individual FC map characteristics

We found significantly increased LI (Feature 1) in low-level ($p = 0.013$) and middle-level ($p = 0.005$) FC maps in patients compared to controls (Feature 1, Fig. 2 and Fig. S2). Patients showed an increased total number of voxels with significant correlation between

the seed and the whole brain (Feature 2) in high-level ($p = 0.022$, Fig. 2). Moreover, the number of voxels in the first cluster (Feature 3, Fig. 2) also showed increased in patients in middle-level ($p = 0.027$) and high-level ($p = 0.005$). The percentage of voxels in the first cluster (Feature 4, Fig. 2) was larger in patients compared with controls in low-level ($p = 0.002$) and middle-level ($p < 0.001$) of FC maps. All these results reflect enhanced local FC in patients. For the 13 patients whose fMRI data included runs with and without IEDs, no significant difference between runs with and without IEDs was found in any of the four features at any of the three threshold levels.

3.4. Overlapping characteristics of FC maps

An increased overlapping characteristic was found in high-level FC maps (Fig. 3). This included an increase in the overlap between individual map and template (Feature 5, $p = 0.018$), an increase in the proportion of overlapping voxels (Feature 6, $p = 0.003$), and a higher proportion of non-overlapping voxels (Feature 7, $p = 0.022$), when comparing patients to controls. No significant difference was found in low- and middle-level FC maps between patients and controls. These results reflect that connections from high-level threshold in patients are enhanced in regions overlapping with the template as well as in individual non-overlapping regions. For the 13 patients with runs with and without IEDs, we only found increased overlap between individual map and template (Feature 5, $p = 0.042$) and the proportion of overlapping voxels (Feature 6, $p = 0.024$) in the case with IEDs in contrast to the case without IEDs in low-level FC maps. No significant difference was found in individual non-overlapping ratio between the two cases.

At the cluster level, an increased percentage of overlapping voxels located in the first cluster (Feature 8) was found in low-level ($p < 0.001$) and middle-level ($p = 0.003$) FC maps in patients compared to controls (Fig. 4). This result implies that the overlapping voxels are mainly included in the first overlapping cluster in patients. The proportion of overlapping voxels outside the first cluster (Feature 9) was significantly decreased in patients compared to controls at all three threshold levels [$p < 0.001$ (low), $p < 0.001$ (middle), and $p = 0.04$ (high), Fig. 4]. This reflects reduced distant overlapping clusters in patients. For the 13 patients whose fMRI data included runs with and without IED, no significant difference was found in the two features at any threshold level.

In Fig. 5, an example from a patient is shown. This patient has focal cortical dysplasia in the left superior frontal gyrus. The seed was identified in the left superior frontal gyrus because the maximum activation was found in this region in EEG/fMRI. The normal FC map (template) was obtained in controls with the left superior frontal gyrus as seed. This map included the bilateral medial frontal cortex, superior frontal gyrus, posterior cingulate cortex, angular gyrus, middle temporal gyrus, left caudate nucleus, left frontal operculum and left middle frontal gyrus. Most of these regions are part of the default mode network (DMN). The three level FC maps of the patient are overlapped on the control template in Fig. 5. At the high-level, the overlap was observed at the left superior frontal gyrus (first cluster). The non-overlapping cluster of the patient's map was located in the middle cingulate cortex, bilaterally. At the middle-level, the overlap was observed at the left superior frontal gyrus (first cluster) and left frontal operculum (distant region). The non-overlapping clusters of the patient's map included the left insula, bilateral thalamus, and brain stem, besides those in high-level map. At the low-level, the overlap added another distant region, the right superior frontal gyrus, and the non-overlapping clusters also increase compared to the middle-level, such as the right insula. In all three level maps, the posterior regions of the control template, such as the posterior cingulate cortex and angular gyrus, never overlapped with the patient's map. These findings imply that the seed at the left superior frontal gyrus links to the bilateral middle cingulate cortex, thalamus and insula in this patient, but mostly to the DMN in controls. Besides, it should be mentioned that the extent of the difference between connection patterns in patients and control subjects varies across patients. Because the seeds in patients are different from each other, after we reviewed all patient patterns, we could not find common areas of seizure propagation in this FLE group. Additional figures from three patients are shown in the Supplementary figures (Figs. S3, S4 and S5).

3.5. Individual variance of FC map

After dividing the CCs into a patient group (between PA-S*m* and HC*n*-S*m*) and a control group (between HC*n*-S*m*), the averaged CC of the patient group was 0.331, and that of the control group was 0.357. The lower CC for the patient group, which suggests a higher variance, was found with marginal significance when compared to controls ($t = 1.33$, $p = 0.09$). The correlation between the variance (the averaged CC between PA-S*m* and HC*n*-S*m*) and the 9 FC map features was evaluated in the patient group separately. We did not find a significant relationship between the variance and those features in patients. In other words, the variance of FC map might not significantly influence the findings in the 9 features evaluated here.

4. Discussion

In the current study, we use FC analysis to delineate the FC pattern related to the potential epileptogenic region, as identified by the IED-related activation of EEG/fMRI analysis. Through the comparisons of multiple features in FC patterns between patients with IEDs and healthy controls, three major findings were observed. First, we found more functional connections between the potential epileptogenic region and the whole brain, and more predominantly unilateral FC maps in patients compared to controls. Second, the neighborhood of the seed region (epileptogenic region) showed enhanced FC in the patients compared to the FC of the same region in the controls, as measured by first cluster FC and by first cluster overlap features. Finally, we found a decrease in FC between the focus and remote regions, as measured by a decrease in significant voxels located outside the first overlapping clusters. Patients also showed increased individual non-overlapping regions in high-level connections (CC > 0.7). These findings imply a patient-specific connectivity pattern of the epileptic network in FLE, which could be thought of as characterized by high connectivity around the focus and patient-specific distant connection. The abnormally high connectivity might reflect a predominant attribute of the epileptic network, which may facilitate propagation of epileptic activity among regions in the network. These findings supported our hypothesis that the FC patterns related to the epileptogenic region were different from the general connectivity pattern in control subjects.

The connectivity analysis based on connectivity between a seed and the whole brain is probably the most common approach to examine FC in the brain. How to choose the seed is critical in this approach. Previous studies suggested that EEG/fMRI could provide valuable information for pre-surgical evaluation (Zijlmans et al., 2007; Thornton et al., 2010; Elshoff et al., 2012). Recently, our study showed that the IED-related activation with t-max could help localize the epileptogenic region and predict the surgical outcome in focal epilepsy (An et al., 2013). According to these observations, we choose the IED-related activation with t-max in frontal lobe as a seed to delineate the epileptic focus. The FC map could reflect the epileptic activity and potential propagation pathways in FLE. Using FC analysis with a seed at the overlap between the IED-related activation cluster and the planned resection area, Negishi et al. (2011) revealed higher lateral pre-surgery FC maps in intractable patients with good surgical outcome (seizure-free at 1-year follow-up) compared to those with poor outcome (seizure recurrence). In line with their findings, we find lateralized FC distribution in FLE compared with controls.

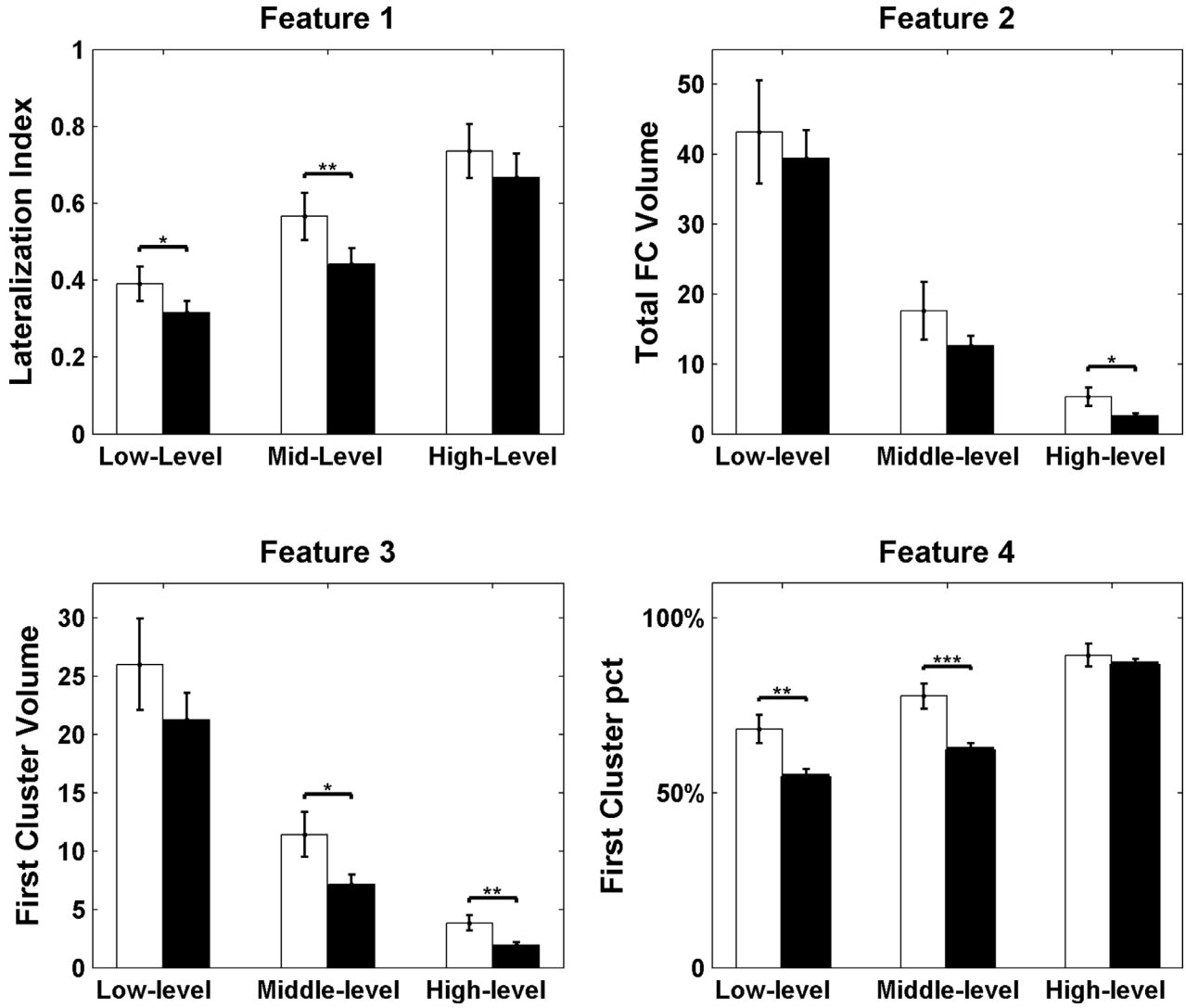

Fig. 2. Individual FC map characteristics. Feature 1, lateralization index of FC map; Feature 2, total FC volume normalized by the size of seed; Feature 3, first cluster volume normalized by the size of seed; and Feature 4, the first cluster percentage relative to the individual total FC. The white bar shows the results for patients, and the black bar the results for controls. The error bar represents the standard error. $^{*}p < 0.05$, $^{**}p < 0.01$, $^{***}p < 0.001$.

Epileptic seizures reflect abnormal neuronal synchronization, and the concept of network has been used to delineate the alteration of synchronization in epilepsy. In previous studies, we and others showed decreased FC in the epileptic network in TLE (Morgan et al., 2012; Pittau et al., 2012). This pathology is different from that of our patients because it consists mostly of atrophy and cell loss, which could easily lead to decreased FC. Our patients show a disorganized cortex but not necessarily cell loss. We did not evaluate the connectivity strength between groups in the current study because varied focus localizations in a group of FLE patients lead to different seeds (the centers of gravity of the 25 seeds are different). Our findings demonstrate that the abnormalities in FC of the epileptogenic region are local and unilateral in FLE. In particular, the volume of local FC (the first FC cluster) is significantly larger than that in controls in the high-level connection threshold situation. The high-level correlation threshold, larger than 0.7, is not a common choice in FC studies because it results in sparse connectivity. However, a high threshold may help reveal regions of high synchrony. Our finding may therefore imply that the focus may lead to an extension of the region with high synchrony in the BOLD signal.

FC results are generally presented as a stable statistical map computed across a group of subjects, such as the DMN and motor network. We adopted a group-level FC map in a large group of controls as a template to delineate the FC pattern at a given seed. We observe that patients show more overlapping voxels in the first overlapping cluster at low- and middle-level threshold FC maps. The significant difference between two groups is absent in the high-level case possibly because of the highly localized high-level FC for each subject. This implies that patients have a more highly connected region around the focus, but less connection with distant regions (non-first overlapping clusters) in FC of control subjects. Moreover, we find more non-overlapping voxels with the template in the patient group compared to controls, when using high-level threshold for the maps. For the example shown in Fig. 5 and Figs. S3–5, the middle cingulate cortex, thalamus and insula represent the patient-specific regions connected with the seed region. This result may reflect that these regions with high synchrony are present in patient-specific connections, and absent in control subjects. Taken together, our findings are consistent with our hypothesis of the presence of a patient-specific network. We presume that the patient-specific network might facilitate propagation of epileptic activity.

In addition, for the 13 patients whose fMRI data included runs with and without IED, we only found increased total overlapping volume and total overlapping ratio to the template in low-level FC map in the

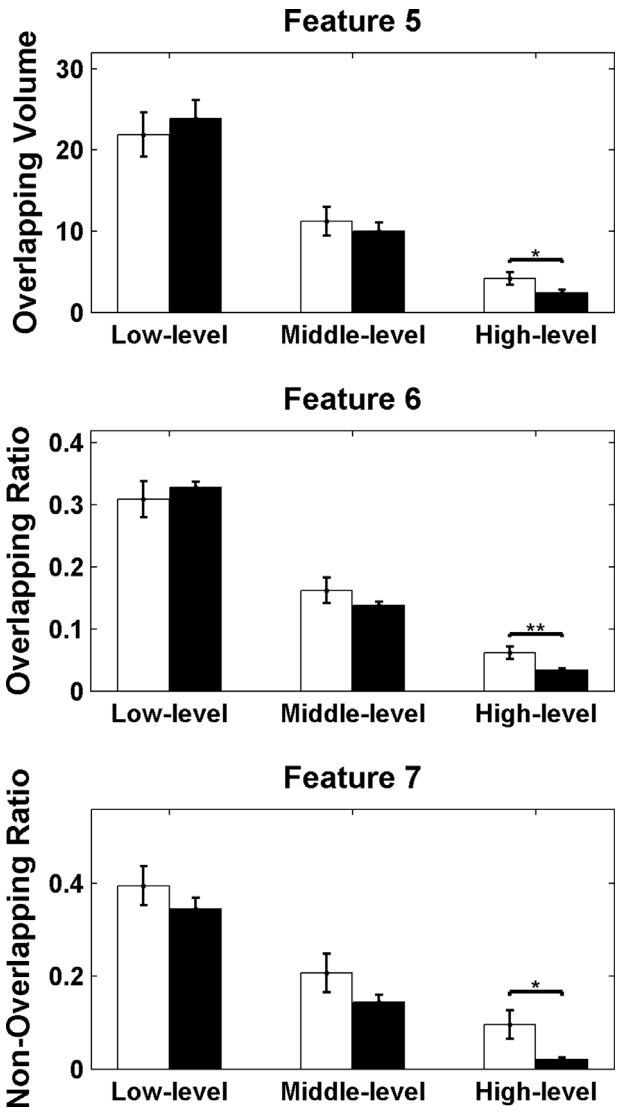

Fig. 3. Overlap characteristics between the individual FC maps and the template. Feature 5, overlap between individual map and template; Feature 6, proportion of overlapping voxels; Feature 7, proportion of non-overlapping voxels. The white bar shows the results for patients, and the black bar the results for controls. The error bar represents the standard error. $^{*}p < 0.05$, $^{**}p < 0.01$.

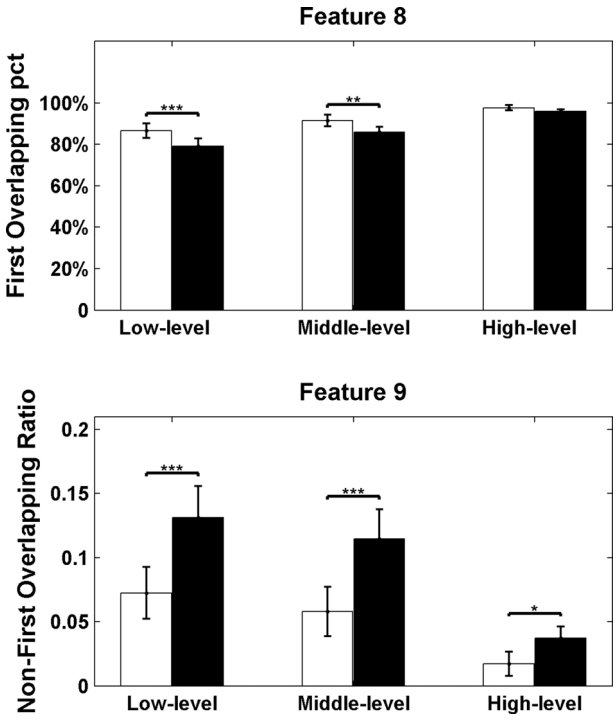

Fig. 4. Cluster-level overlap characteristics. Feature 8, percentage overlapping voxels located in the first cluster; Feature 9, proportion of overlapping voxels outside the first cluster. The differences between two groups with (patients and healthy controls) were significant ($p < 0.05$), as revealed by the p values. White bars show the results of the patient group, and black bars show the results of controls. Error bars represent the standard error. $^{*}p < 0.05$, $^{**}p < 0.01$, $^{***}p < 0.001$.

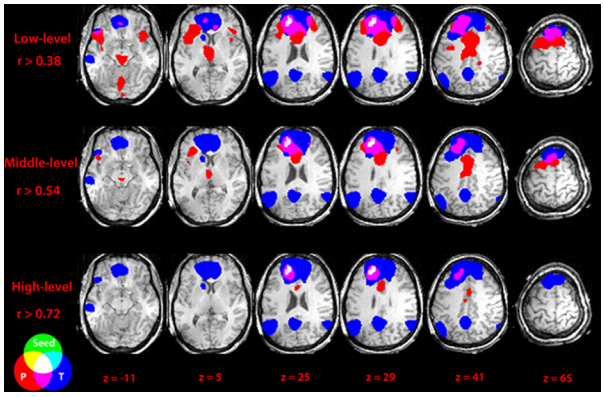

Fig. 5. Example of overlapping FC for a patient. The green represents the seed. The red represents the FC map in the patient and the blue represents the FC template from healthy controls with the same seed. The circles at the bottom left show how the colors overlap. Abbreviation: P, FC map of patient, and T, template. The patient's connectivity pattern is very different from that of the control group.

group of runs with IED compared to the group of runs without IED. These findings demonstrate that interictal epileptic activity does not influence the features of the epileptic network at a high-level of FC.

The frontal lobe shows functional variability because it is associated with various higher-order cognitive abilities (Mueller et al., 2013). The group-level result of FC seeded in the frontal lobe should be carefully interpreted. In the current study, we try to delineate individual FC pattern features rather than the strength of FC across voxels. To some extent, the individual variability leads to our results. For example, the overlapping characteristics, which were evaluated for each subject, reflect the presence of individual variability. Moreover, lower spatial correlation was found between FC maps of patients and controls when compared to that among controls (marginal significance, $p = 0.09$). This would help support a partly patient-specific connectivity pattern. Finally, antiepileptic drugs may affect functional connectivity in the brain. In the current study, all patients took medication but with such variability of medication, combination of medications, and doses that it would be impossible to assess the specific effect of a medication. Drug-naïve patients should be investigated in the future.

In summary, our study suggests a patient-specific connectivity pattern of epileptic network in FLE, characterized by high local connectivity and specific distant connections. We provide the abnormal characteristics of epileptic network patterns to support the patient-specific network in focal epilepsy. The altered FC pattern with high local connectivity could be considered an attribute of epileptic networks, which may facilitate the generation of intense local epileptic activity. We also speculate that the special alteration of local high connectivity might help localize epileptogenic regions in focal epilepsy.

Conflicts of interest

None of the authors has any conflict of interest to disclose. We confirm that we have read the Journal's position on issues involved in ethical publication and affirm that this report is consistent with those guidelines.

Acknowledgments

This project was funded by grants from the 973 Project 2011CB707803, the National Nature Science Foundation of China (81271547, 81160166, 81100974, 81071222, and 91232725). This work was also supported by the Canadian Institutes of Health Research (MOP-38079). The authors thank Natalja Zazubovits for helping to collect and analyze the data, and Dr. Mouna Safi-Harb for her comments about the methods and the English language.

Appendix A. Supplementary materials

Supplementary material associated with this article can be found, in the online version, at http://dx.doi.org/10.1016/j.nicl.2014.04.007.

References

An, D., et al. 2013. Electroencephalography/functional magnetic resonance imaging responses help predict surgical outcome in focal epilepsy. Epilepsia 54 (12), 2184–94. http://dx.doi.org/10.1111/epi.12434, 24304438.

Bagshaw, A.P., et al. 2004. EEG–fMRI of focal epileptic spikes: analysis with multiple haemodynamic functions and comparison with gadolinium-enhanced MR angiograms. Human Brain Mapping 22 (3), 179–92. http://dx.doi.org/10.1002/hbm.20024, 15195285.

Benar, C., et al. 2003. Quality of EEG in simultaneous EEG–fMRI for epilepsy. Clinical Neurophysiology: Official Journal of the International Federation of Clinical Neurophysiology 114 (3), 569–80. http://dx.doi.org/10.1016/S1388-2457(02)00383-8, 12705438.

Bettus, G., et al. 2009. Decreased basal fMRI functional connectivity in epileptogenic networks and contralateral compensatory mechanisms. Human Brain Mapping 30 (5), 1580–91. http://dx.doi.org/10.1002/hbm.20625, 18661506.

Biswal, B., et al. 1995. Functional connectivity in the motor cortex of resting human brain using echo-planar *MRI*. Magnetic Resonance in Medicine: Official Journal of the Society of Magnetic Resonance in Medicine / Society of Magnetic Resonance in Medicine 34 (4), 537–41. http://dx.doi.org/10.1002/mrm.1910340409, 8524021.

Constable, R.T., et al. 2013. Potential use and challenges of functional connectivity mapping in intractable epilepsy. Frontiers in Neurology 4, 39, 23734143.

Elshoff, L., et al. 2012. The value of EEG–fMRI and EEG source analysis in the presurgical setup of children with refractory focal epilepsy. Epilepsia 53 (9), 1597–606. http://dx.doi.org/10.1111/j.1528-1167.2012.03587.x, 22779700.

Engel, J. Jr., 2001. A proposed diagnostic scheme for people with epileptic seizures and with epilepsy: report of the ILAE Task Force on Classification and Terminology. Epilepsia 42 (6), 796–803. http://dx.doi.org/10.1046/j.1528-1157.2001.10401.x, 11422340.

Fahoum, F., et al. 2012. Widespread epileptic networks in focal epilepsies: EEG–fMRI study. Epilepsia 53 (9), 1618–27. http://dx.doi.org/10.1111/j.1528-1167.2012.03533.x, 22691174.

Friston, K.J., et al. 1994. Assessing the significance of focal activations using their spatial extent. Human Brain Mapping 1 (3), 210–20, 24578041.

Kramer, M.A., Cash, S.S., 2012. Epilepsy as a disorder of cortical network organization. Neuroscientist: A Review Journal Bringing Neurobiology, Neurology and Psychiatry 18 (4), 360–72. http://dx.doi.org/10.1177/1073858411422754, 22235060.

Laufs, H., 2012. Functional imaging of seizures and epilepsy: evolution from zones to networks. Current Opinion in Neurology 25 (2), 194–200. http://dx.doi.org/10.1097/WCO.0b013e3283515db9, 22322414.

Liao, W., et al. 2011. Default mode network abnormalities in mesial temporal lobe epilepsy: a study combining fMRI and *DTI*. Human Brain Mapping 32 (6), 883–95. http://dx.doi.org/10.1002/hbm.21076, 20533558.

Luo, C., et al. 2011. Altered functional connectivity in default mode network in absence epilepsy: a resting-state fMRI study. Human Brain Mapping 32 (3), 438–49. http://dx.doi.org/10.1002/hbm.21034, 21319269.

Luo, C., et al. 2012. Resting state basal ganglia network in idiopathic generalized epilepsy. Human Brain Mapping 33 (6), 1279–94. http://dx.doi.org/10.1002/hbm.21286, 21520351.

Maneshi, M., et al. 2012. Resting-state connectivity of the sustained attention network correlates with disease duration in idiopathic generalized epilepsy. PloS One 7 (12), e50359. http://dx.doi.org/10.1371/journal.pone.0050359, 23227168.

Morgan, V.L., et al. 2012. Lateralization of temporal lobe epilepsy using resting functional magnetic resonance imaging connectivity of hippocampal networks. Epilepsia 53 (9), 1628–35. http://dx.doi.org/10.1111/j.1528-1167.2012.03590.x, 22779926.

Mueller, S., et al. 2013. Individual variability in functional connectivity architecture of the human brain. Neuron 77 (3), 586–95. http://dx.doi.org/10.1016/j.neuron.2012.12.028, 23395382.

Negishi, M., et al. 2011. Functional MRI connectivity as a predictor of the surgical outcome of epilepsy. Epilepsia 52 (9), 1733–40. http://dx.doi.org/10.1111/j.1528-1167.2011.03191.x, 21801165.

Pittau, F., Dubeau, F., Gotman, J., 2012. Contribution of EEG/fMRI to the definition of the epileptic focus. Neurology 78 (19), 1479–87. http://dx.doi.org/10.1212/WNL.0b013e3182553bf7, 22539574.

Pittau, F., et al. 2012. Patterns of altered functional connectivity in mesial temporal lobe epilepsy. Epilepsia 53 (6), 1013–23. http://dx.doi.org/10.1111/j.1528-1167.2012.03464.x, 22578020.

Thornton, R., et al. 2010. EEG correlated functional MRI and postoperative outcome in focal epilepsy. Journal of Neurology, Neurosurgery, and Psychiatry 81 (8), 922–7. http://dx.doi.org/10.1136/jnnp.2009.196253, 20547617.

Vaessen, M.J., et al. 2013. Abnormal modular organization of functional networks in cognitively impaired children with frontal lobe epilepsy. Cerebral Cortex (New York, N.Y.: 1991) 23 (8), 1997–2006. http://dx.doi.org/10.1093/cercor/bhs186, 22772649.

Zhang, Z., et al. 2011. Altered functional–structural coupling of large-scale brain networks in idiopathic generalized epilepsy. Brain: A Journal of Neurology 134 (10), 2912–28. http://dx.doi.org/10.1093/brain/awr223, 21975588.

Zijlmans, M., et al. 2007. EEG–fMRI in the preoperative work-up for epilepsy surgery. Brain: A Journal of Neurology 130 (9), 2343–53. http://dx.doi.org/10.1093/brain/awm141, 17586868.